Free vibration of a thin spherical shell containing a compressible fluid

Mingsian R. Bai and Kuorung Wu
Department of Mechanical Engineering, National Chiao Tung University, Hsin Chu 30050, Taiwan, Republic of China

(Received 28 April 1993; revised 22 November 1993; accepted 18 January 1994)

Free vibration of a thin spherical shell filled with a compressible fluid is investigated. The interactions at the interface between the elastic structure and the compressible fluid are taken into account. The objective of this study is to develop a hybrid numerical technique for the free vibration analysis of sound–structure interaction problems. The boundary element method is employed for modeling the acoustic disturbances in the cavity, while the finite element method is used for modeling the structural dynamics of the shell. The formulations are then combined into a coupled numerical scheme for the total pressure-displacement field. Natural frequencies and mode shapes are calculated by using the singular value decomposition algorithm. Physical insights into the resonance phenomena associated with sound–structure interactions are derived from the comparison between the results of the thin spherical shell, with and without the fluid loading effect.

PACS numbers: 43.40.Ey

INTRODUCTION

For an elastic structure filled with a compressible fluid, interactions exist between the acoustic field of the fluid and the vibration field of the structure. In most cases, the dynamic response of a structure in contact with a fluid can be determined as if the structure were vibrating *in vacuo* because the radiation loading exerted by the fluid is generally small enough to have a negligible effect on the structural vibrations. Radiation loading significantly modifies the motion of a structure only under exceptional circumstances, e.g., when a volume of air is confined in a small enclosure, when the structure is relatively light, or when an elastic structure is submerged in a heavy fluid. On these occasions, the elastic structure and the acoustical field cannot be treated as uncoupled systems and must be solved simultaneously.

There has been ongoing research on the subject of sound–structure interactions. To name a few, the sound–structure interaction problem was explored by Faran in 1951 who used the method of separation of variables to derive closed form solutions for acoustic fields scattered by elastic solid cylinders and spheres.[1] Then, Junger used an analytical approach to solve acoustic fields scattered by thin elastic shells.[2] Instead of analytical approaches, Chen and Schweikert applied numerical methods to analyze fluid–structure interactions for arbitrarily shaped bodies submerged in an infinite medium.[3] In 1977, Zienkiewicz, Kelly, and Bettess proposed a finite element method (FEM)–based formulation for coupled systems.[4] Then, Wilton solved an exterior fluid–structure interaction problem by coupling the boundary element method (BEM) and the FEM.[5] More recently, an analysis was presented by Wu for analyzing radiation and scattering problems associated with submerged elastic axisymmetric bodies.[6]

The aforementioned research efforts all fall into the category of exterior problems when the structures are submerged in fluids. This does not preclude the importance of interior sound–structure interaction problems, where the structures may contain fluids in their interiors. There are many situations in which the interior problems of sound–structure interactions may be of importance, such as ramjet engines, nuclear reactors, and pressure vessels. Although the literature concerning the interior problems of sound–structure interactions is not as ample as that of the exterior counterpart, similar numerical techniques can still be applied to calculate the total response of a containing elastic structure. Of particular interest in this study is the development of a *hybrid* numerical method for the free vibration analysis of structures filled with compressible fluids. While the numerical technique is developed in a rather general form, a thin spherical shell container is chosen in the simulation to verify the algorithm not only because it interacts more strongly with the contained fluid compared with the thick shell, but also because its analytical solution is more tractable than the other odd-shaped structures. Nevertheless, the numerical simulation is conducted without taking the advantages of symmetry. The method developed thus can be applied to problems of arbitrary geometries where analytical solutions are in general not available.

The objective of this research is twofold: first, to demonstrate the implementation of the coupled FEM–BEM technique; and, second, to explore the sound–structure interaction behavior via an extensive numerical simulation. The free vibration analysis has three steps. First, the acoustic field enclosed by a rigid spherical boundary is analyzed by BEM. Next, the free vibration of a thin spherical shell *in vacuo* is analyzed by FEM. Finally, the free vibration of the containing thin spherical shell subjected to loading effects is analyzed by the coupled BEM–FEM technique. An algorithm based on singular value decomposition (SVD) is

 0001-4966/94/95(6)/3300/11/$6.00

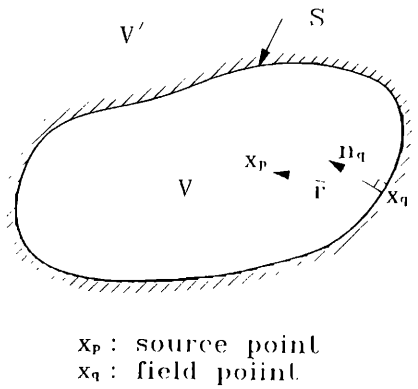

FIG. 1. Schematic diagram for an interior boundary value problem of the acoustic field in an enclosure.

developed for efficiently searching for the natural frequencies and mode shapes of the coupled system. Physical insights are derived from the results of the spherical shell with and without the fluid loading.

I. ANALYSIS OF THE ACOUSTICAL SYSTEM

From the theory of linear acoustics, a monochromatic sound field in an inviscid and compressible fluid is described by the Helmholtz equation[7]

$$(\nabla^2+k^2)p(\mathbf{x})=0, \tag{1}$$

where $k=\omega/c$ is the wave number (ω and c are, respectively, the angular frequency and the speed of sound). The radius of the spherical enclosure is a. The interior acoustic field has the general solution

$$p(\mathbf{x},n,m)=[A_{nm}\cos(m\phi) + B_{nm}\sin(m\phi)]P_n^m(\cos\theta)j_n(kr), \tag{2}$$

where A_{nm} and B_{nm} are arbitrary constants to be determined by boundary conditions, P_n^m is the associated Legendre polynomial ($m\leqslant n$), and j_n is the spherical Bessel function of the first kind of order n.

Alternatively, the solution of the interior boundary value problem of the acoustic field of Fig. 1 can be expressed as the Kirchhoff–Helmholtz integral

$$\alpha(\mathbf{x}_p)p(\mathbf{x}_p)=\int_S\left(G(\mathbf{x}_p,\mathbf{x}_q)\frac{\partial}{\partial n_q}p(\mathbf{x}_q) - p(\mathbf{x}_q)\frac{\partial}{\partial n_q}G(\mathbf{x}_p,\mathbf{x}_q)\right)dS, \tag{3}$$

where

$$a(\mathbf{x}_p)=\begin{cases}1, & \mathbf{x}_p\in V,\\ \Omega(\mathbf{x}_p)/4\pi, & \mathbf{x}_p\in S\\ 0, & \mathbf{x}_p\in V'\end{cases}$$

[$\Psi(\mathbf{x}_p)$ is the solid angle at the point $\mathbf{x}_p$],[8] $G(x_p,x_q)=\exp(ikr)/4\pi r$ is the free-space Green's function, the position vectors $\mathbf{x}_p$ and $\mathbf{x}_q$ denote the field point and the source point, respectively, the distance $r=|\mathbf{x}_p-\mathbf{x}_q|$, and the directional directive $\partial/\partial n_q\equiv\mathbf{n}_q\cdot\nabla$ with $\mathbf{n}_q$ being the outward normal to the surface S.

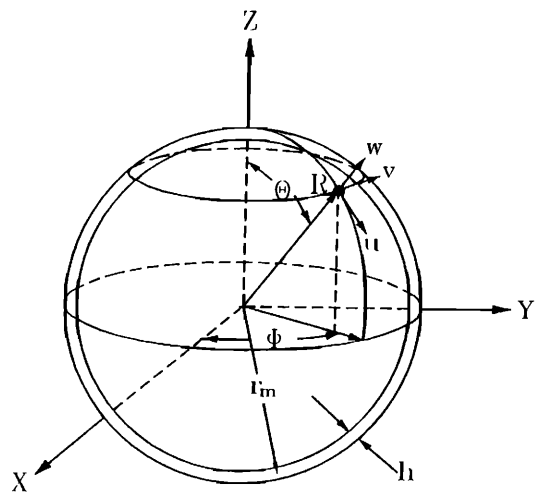

FIG. 2. The thin spherical shell and spherical coordinates.

With the field point taken to the boundary S, Eq. (3) becomes a boundary integral equation, which can further be discretized into a matrix form[9]

$$\mathbf{AP}-\mathbf{BP}_n=\mathbf{0}, \tag{4}$$

where $\mathbf{P}$ is the acoustic pressure vector and $\mathbf{P}_n$ is the acoustic pressure gradient vector. Here, Eq. (4) constitutes the main equation for the acoustical subsystem. For some subtle points involved in the numerical implementation, such as fictitious frequencies, nonsmooth boundaries, and singular elements, one may consult the related literature (e.g., Ref. 9).

II. ANALYSIS OF THE STRUCTURAL SYSTEM

A. Analytical solution of the thin spherical shell *in vacuo*

Consider a thin spherical shell of thickness h and radius r_m ($h\ll r_m$), as shown in Fig. 2, with the material properties: the mass density ρ_s, the Young's modulus E, and Poisson's ratio ν. From the Love–Kirchhoff theory[10–12] of thin shells, the simplified shell equations for monochromatic motions based on axisymmetry are

$$L_{uu}u+L_{uw}w+\Omega^2u=0, \tag{5}$$

$$L_{wu}u+L_{ww}w+\Omega^2w=-q(1-\nu^2)r_m^2/Eh, \tag{6}$$

where the nondimensional frequency $\Omega^2=\omega^2r_m^2/c_p^2$, $c_p=[E/(1-\nu^2)\rho_s]^{1/2}$ is the phase velocity of compressible waves, q is the normal stress acting on the middle surface, and the differential operators L_{uu}, L_{uw}, L_{wu}, and L_{ww} are defined as

$$L_{uu}=(1+\gamma^2)\left((1-\eta^2)^{1/2}\frac{d^2}{d\eta^2}(1-\eta^2)^{1/2}+(1-\nu)\right), \tag{7}$$

$$L_{uw}=(1-\eta^2)^{1/2}\left([\gamma^2(1-\nu)-(1+\nu)]\frac{d}{d\eta}+\gamma^2\frac{d}{d\eta}\nabla_\eta^2\right), \tag{8}$$

$$L_{wu}=-\left([\gamma^2(1-\nu)-(1+\nu)]\frac{d}{d\eta}(1-\eta^2)^{1/2}+\gamma^2\nabla_\eta^2\frac{d}{d\eta}(1-\eta^2)^{1/2}\right), \tag{9}$$

$$L_{ww}=-\gamma^2\nabla_\eta^4-\gamma^2(1-\nu)\nabla_\eta^2-2(1+\nu), \tag{10}$$

with

$$\gamma^2=\frac{h^2}{12r_m^2},\quad \nabla_{\theta\phi}^2=\frac{1}{\sin\theta}\frac{\partial}{\partial\theta}\left(\sin\theta\frac{\partial}{\partial\theta}\right)+\frac{1}{\sin^2\theta}\frac{\partial^2}{\partial\phi^2},\quad \nabla_\eta^2=\frac{d}{d\eta}(1-\eta^2)\frac{d}{d\eta}. \tag{11}$$

The free vibration of the spherical shell can be analyzed in terms of $P_n(\eta)$, the Legendre polynomial of the first kind of order n:

$$u(\eta)=\sum_{n=0}^{\infty}U_n(1-\eta^2)^{1/2}\frac{dP_n(\eta)}{d\eta}, \tag{12}$$

$$w(\eta)=\sum_{n=0}^{\infty}W_nP_n(\eta). \tag{13}$$

Hence, the expansion coefficients U_n and W_n must satisfy the relations

$$[\Omega^2-(1+\gamma^2)(\nu+\lambda_n-1)]U_n-[\gamma^2(\nu+\lambda_n-1)+(1+\nu)]W_n=0, \tag{14}$$

$$\lambda_n[\gamma^2(\nu+\lambda_n-1)+(1+\nu)]U_n-[\Omega^2-2(1+\nu)-\gamma^2\lambda_n(\nu+\lambda_n-1)]W_n=0, \tag{15}$$

where $\lambda_n=n(n+1)$. The determinant of the coefficients must vanish for nontrivial solutions of the unknowns U_n and W_n. This leads to the frequency equation

$$\Omega^4-[1+3\nu+\lambda_n+\gamma^2(\lambda_n+1)(\lambda_n-1+\nu)]\Omega^2-(\lambda_n-2)(1-\nu^2)+\gamma^2(\lambda_n-2)[(\lambda_n-1)^2-\nu^2]=0. \tag{16}$$

Each mode associated with an index $n>0$ corresponds to two distinct branches of resonant frequencies. However, for $n=0$ corresponding to what is called the *breathing mode*, only one real frequency exists. On the other hand, for nonaxisymmetric torsional modes, another frequency equation reads

$$\Omega^2-\Omega_n^2=0, \tag{17}$$

where $\Omega_n=[\frac{1}{2}(n+2)(n-1)(1+\gamma^2)(1-\nu)]^{1/2}$.

B. The numerical method (FEM)

Standard FEM formulation of an elastic structure yields the matrix equation for harmonic motions,[13]

$$(\mathbf{K}+i\omega\mathbf{C}-\omega^2\mathbf{M})\mathbf{U}=\mathbf{R}, \tag{18}$$

where **K**, **C**, and **M** are, respectively, the stiffness matrix, damping matrix, and mass matrix; **R** is the external force vector; and **U** is the displacement vector. The matrices **K**, **C**, **M**, and **R** are assembled from the matrix for the element e as[13]

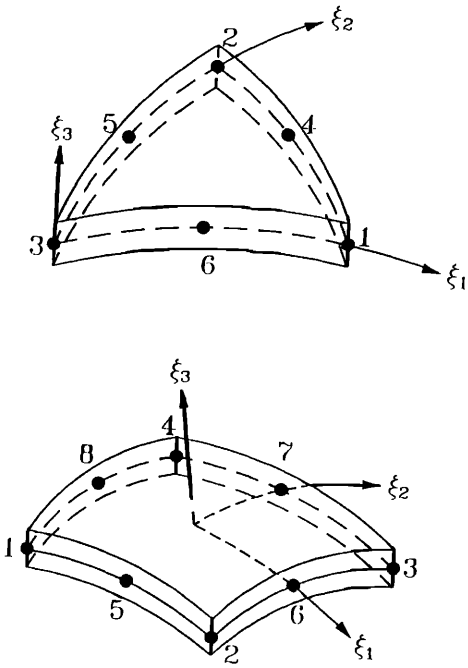

FIG. 3. The six-node and eight-node degenerate shell elements.

$$\mathbf{K}=\sum_e\mathbf{K}^{(e)}=\sum_e\int_{V^{(e)}}\tilde{\mathbf{B}}^t\mathbf{E}\tilde{\mathbf{B}}\,dV, \tag{19}$$

$$\mathbf{C}=\sum_e\mathbf{C}^{(e)}=\sum_e\int_{V^{(e)}}\mu\bar{\mathbf{N}}^t\bar{\mathbf{N}}\,dV, \tag{20}$$

$$\mathbf{M}=\sum_e\mathbf{M}^{(e)}=\sum_e\int_{V^{(e)}}\rho_s\bar{\mathbf{N}}^t\bar{\mathbf{N}}\,dV, \tag{21}$$

and

$$\mathbf{R}=\sum_e\mathbf{R}^{(e)}=\sum_e\int_{V^{(e)}}\bar{\mathbf{N}}^t\mathbf{b}\,dV+\sum_e\int_{S^{(e)}}\bar{\mathbf{N}}^t\mathbf{q}\,dS+\sum_{i=1}^{n}\mathbf{F}_i, \tag{22}$$

in which $\tilde{\mathbf{B}}$ is the strain-displacement matrix, **E** is the stress-strain matrix, $\bar{\mathbf{N}}$ is the shape function matrix, **b** is the body force vector, **q** is the traction vector, $\mathbf{F}_i$ is the concentrated force vector, and ρ_s and μ are the mass density and damping factor of the structure, respectively.

In principle, a three-dimensional elasticity problem can be modeled by solid elements that are, unfortunately, not suited for the thin shell considered here because of its exceedingly large aspect ratios.[14] In fact, spherical shell elements happen to be among the structural elements the most difficult elements to design in implementing FEM codes. Special types of six- and eight-node degenerate curved shell elements in Fig. 3 are thereby employed for the analysis of the thin spherical shell. The details can be found in Refs. 15 and 16.

III. FREE VIBRATION ANALYSIS OF THE COUPLED SYSTEM

A. Analytical solution of the coupled system

A modal matching method is used for obtaining the analytical solution of the coupled fluid–shell system. Consider the forced vibration of the thin spherical shell subjected to a harmonic excitation pressure $q=f(\eta)\exp(i\omega t)$, which can be expanded in terms of the Legendre polynomials $P_n(\eta)$ as

$$f(\eta)=\sum_{n=0}^{\infty} f_n P_n(\eta). \tag{23}$$

Substituting Eq. (23) into the equations of motion (5) and (6) gives

$$[\Omega^2-(1+\gamma^2)(\nu+\lambda_n-1)]U_n - [\gamma^2(\nu+\lambda_n-1)+(1+\nu)]W_n=0, \tag{24}$$

$$\lambda_n[\gamma^2(\nu+\lambda_n-1)+(1+\nu)]U_n - [\Omega^2-2(1+\nu)-\gamma^2\lambda_n(\nu+\lambda_n-1)]W_n = [(1-\nu^2)r_i^2/Eh]f_n. \tag{25}$$

For the sound–structure interaction problem, the excitation pressure q should be replaced by the negative of interface acoustic pressure $-p_i$:

$$p_i=\sum_{n=0}^{\infty} i\omega z_n W_n|_{r=r_i}, \tag{26}$$

where $z_n = i\rho_f c j_n(kr_i)/j_n'(kr_i)$ denotes the interface acoustic modal impedance. Direct comparison of Eqs. (23) and (26) reveals that $f_n = \rho_f c\omega j_n(kr_i)/j_n'(kr_i)W_n$. Thus the frequency equation turns out to be

$$\left(1+\frac{1}{\omega}\frac{\rho_f c}{\rho_s h}\frac{j_n(kr_i)}{j_n'(kr_i)}\right)\Omega^4 - \left(1+3\nu+\lambda_n-\gamma^2(1-\nu-\lambda_n^2-\nu\lambda_n) + \frac{1}{\omega}\frac{\rho_f c}{\rho_s h}\frac{j_n(kr_i)}{j_n'(kr_i)}(1+\gamma^2)(\lambda_n-1+\nu)\right)\Omega^2 - (\lambda_n-2)(1-\nu^2)+\gamma^2(\lambda_n-2)[(\lambda_n-1)^2-\nu^2]=0. \tag{27}$$

The natural frequencies Ω of the coupled sound–structure system can be solved by iteration methods in conjunction with the solutions of the shell *in vacuo* as the initial guesses.

B. The interface conditions

In order to couple the matrix equations of the acoustical and structural subsystems, the compatibility at the interface must be considered. First, the surface velocity of the structure and the particle velocity of the fluid at the interface along the normal direction must be equal. Second, the normal stress of the elastic structure must equal the acoustic pressure at the interface. The compatibility of velocity and stress in tangential directions at the interface is not imposed because the fluid is assumed to be inviscid.

If the interaction force is treated as the excitation to the structure, Eq. (18) can be modified into

$$(\mathbf{K}+i\omega\mathbf{C}-\omega^2\mathbf{M})\mathbf{U}=\mathbf{R}_{\text{ext}}+\mathbf{R}_{\text{int}}, \tag{28}$$

where $\mathbf{R}_{\text{ext}}$ denotes the externally applied force vector and $\mathbf{R}_{\text{int}}$ denotes an equivalent acoustic force vector acting on the surface of the structure.

The major step of coupling the acoustical and structural subsystems in Eqs. (4) and (28) is accomplished through the use of two coupling matrices $\mathbf{L}$ and $\mathbf{T}$ (Refs. 5 and 17):

$$\mathbf{R}_{\text{int}}=\mathbf{LP} \tag{29}$$

and

$$\mathbf{P}_n=-i\rho_f\omega\mathbf{TU}. \tag{30}$$

The former represents the acoustic pressure and the latter represents the pressure gradient (or, equivalently, the particle velocity) obtained from the Euler's equation along the normal direction at the interface.

C. The coupled system matrices

As mentioned previously, when the interaction between the fluid and the structure is not negligible, the dynamic characteristics of the coupled system must be solved simultaneously. Various approaches can be utilized to form the coupled system equations. One may either substitute the acoustical system equations into the structural system equations (termed the structural variable approach), substitute the structural system equations into the acoustical system equations (termed the acoustical variable approach), or assemble both subsystem equations into a complete set of system equations (termed the mixed variable approach). In this study, the structural variable approach is adopted because it is less computationally expensive than the others. From Eqs. (4), (29), and (30), the interaction force vector can be written as

$$\mathbf{R}_{\text{int}}=-i\rho_f\omega\mathbf{LA}^{-1}\mathbf{BTU}. \tag{31}$$

Then, substituting Eq. (31) into (28) leads to

$$(\mathbf{K}+i\omega\mathbf{C}-\omega^2\mathbf{M}+i\rho_f\omega\mathbf{LA}^{-1}\mathbf{BT})\mathbf{U}=\mathbf{R}_{\text{ext}}. \tag{32}$$

In Eq. (31), let $i\rho_f\omega\mathbf{LA}^{-1}\mathbf{BT}=i\omega\mathbf{R}_d-\omega^2\mathbf{R}_m$ ($\mathbf{R}_d$ and $\mathbf{R}_m$ are the added damping and mass matrices, respectively, which may alter the frequency response of the coupled system[5]). A coupled system equation in terms of structural displacements is then obtained:

$$[\mathbf{K}+i\omega(\mathbf{C}+\mathbf{R}_d)-\omega^2(\mathbf{M}+\mathbf{R}_m)]\mathbf{U}=\mathbf{R}_{\text{ext}}. \tag{33}$$

For undamped free vibrations, the matrix equation of the coupled system obtained from the structural variable approach can be written as

$$[\mathbf{K}-\omega^2(\mathbf{M}+\mathbf{R}_m)]\mathbf{U}=\mathbf{0}. \tag{34}$$

This is the main equation intended for the analysis of the coupled sound–structure system. It should be noted that

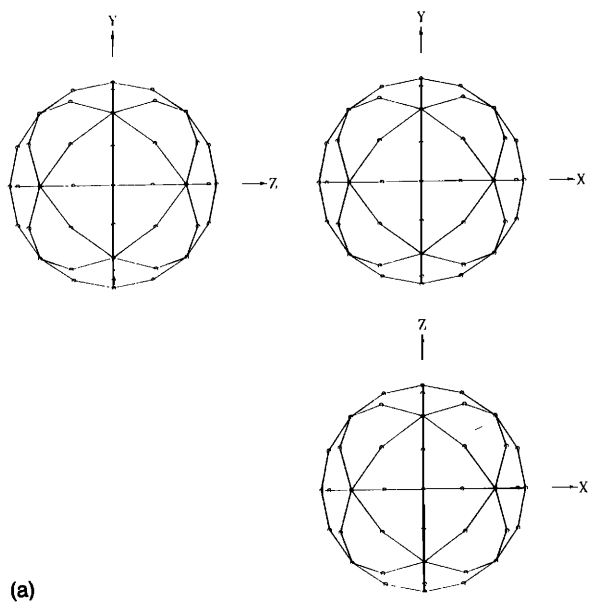

(a)

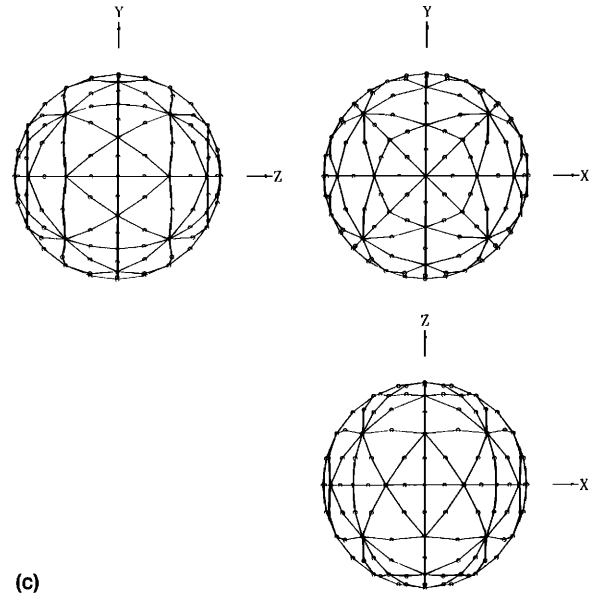

(c)

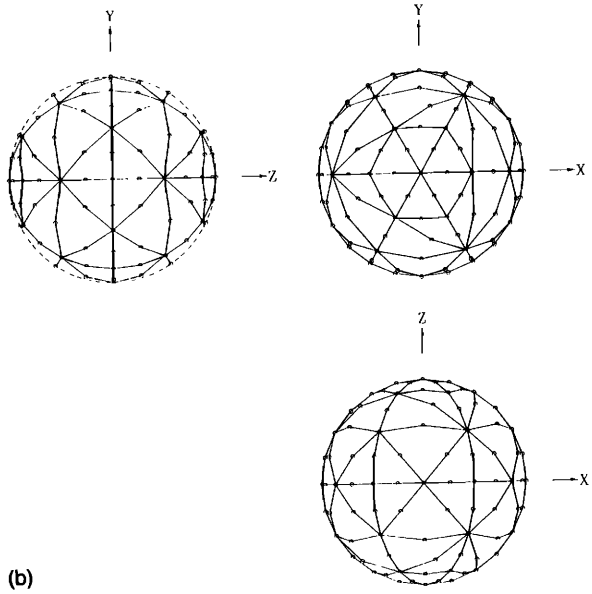

(b)

FIG. 4. The mesh types used in BEM and FEM for the free vibration analysis of the thin spherical shell. (a) Mesh type A (32 elements and 66 nodes); (b) mesh type B (72 elements and 146 nodes); (c) mesh type C (96 elements and 194 nodes).

Eq. (34) is a nonstandard eigenvalue problem since the added mass matrix $\mathbf{R}_m$ is a function of frequency ω.

D. The numerical scheme of searching for natural frequencies and mode shapes

Searching for natural frequencies and mode shapes of the coupled sound–structure system amounts to solving the eigenvalue problem represented by Eq. (34). Frequencies that render the system matrix singular correspond to the eigenvalues and the nontrivial solutions correspond to the eigenvectors. This eigenvalue problem of the coupled system differs from that of the structure *in vacuo* in that the latter is a standard eigenvalue problem $\mathbf{Ax}=\lambda\mathbf{x}$, but the former is not. For such a nonstandard eigenvalue problem, the eigenvalues are embedded in the coefficient matrices, which obviously poses difficulties for ordinary numerical eigenvalue solvers. It is thus desirable to develop a numerical scheme for the eigenvalue analysis of the sound–structure interaction problem. To this end, two approaches termed the method of determinant search and the method of singular value decomposition (SVD) are employed.

Let $\bar{\mathbf{D}}(\omega)=[\mathbf{K}-\omega^2(\mathbf{M}+\mathbf{R}_m)]$. In the method of determinant search, one seeks to determine the eigenvalues by incrementally varying the angular frequency ω such

that the matrix $\bar{\mathbf{D}}(\omega)$ becomes singular. This amounts to finding the angular frequency ω_e, $e=1,2,...$, such that the determinant of $\bar{\mathbf{D}}(\omega)$ vanishes. In practical implementation, one can locate only the local minima of the determinant of $\bar{\mathbf{D}}(\omega)$ for the eigenvalues because it is virtually impossible for $\bar{\mathbf{D}}(\omega)$ to become numerically singular.

On the other hand, the method of SVD involves searching for the frequencies at which the minimum singular value of the coefficient matrix reaches local minima. From linear algebra, the following decomposition of the matrix $\bar{\mathbf{D}}$ exists:[18]

$$\bar{\mathbf{D}}=\mathbf{U}\boldsymbol{\Sigma}\mathbf{V}^h. \tag{35}$$

Here h denotes the Hermitian transpose, $\mathbf{U}$ and $\mathbf{V}$ are both $N\times N$ unitary matrices and are composed of N orthogonal column vectors $\mathbf{u}_i$ and $\mathbf{v}_i$, and $\boldsymbol{\Sigma}$ is a diagonal matrix:

$$\boldsymbol{\Sigma}_{ij}=\begin{cases}\sigma_i\geqslant 0, & i=j,\ \sigma_i\text{'s are singular values,}\\ 0, & \text{otherwise.}\end{cases}$$

If the matrix $\bar{\mathbf{D}}$ is almost singular, then the last one or more singular values must be nearly zero. In order to extract the eigenvalues ω_e, the angular frequency ω is incrementally varied with the step size $\Delta\omega$. Each $\bar{\mathbf{D}}(\omega)$ corresponding to different ω is processed by the SVD algorithm and the minimal singular value σ_n is compared with those obtained from the other iterations. If the minimal singular value σ_n of the matrix $\bar{\mathbf{D}}(\omega)$ reaches a local minimum with respect to the angular frequency ω, then this angular frequency ω is accepted as a desired eigenvalue (although the minimal singular value σ_n may not be numerically zero). Once a possible interval of eigenvalues has been located, optimization schemes such as the Golden section search[19] can then be used to efficiently calculate more accurate eigenvalues. Parallel to searching for eigenvalues, the eigenvectors (or mode shapes) are obtained without additional effort. This is accomplished by a simple observation: Whenever a singular value σ_i vanishes, the right singular vector $\mathbf{v}_i$ of $\bar{\mathbf{D}}$ can be regarded as a legitimate eigenvector. This feature of SVD for finding linearly independent eigenvectors is particularly attractive when there are repeated eigenvalues (which are frequently encountered in problems of high degree of symmetry).

IV. NUMERICAL INVESTIGATIONS

A numerical simulation is undertaken to verify the developed BEM–FEM technique. The dynamic characteristics between the thin spherical shells (with and without the fluid loading) are compared. Quadratic triangular elements are used to construct the mesh on the interface for both the BEM and FEM. The mesh configurations of the BEM and FEM used in the simulation are shown in Fig. 4. The mesh types A, B, and C consist of 32, 72, and 96 elements and 66, 146, and 194 nodes, respectively.

A. The spherical shell *in vacuo*

The free vibration of the thin spherical shell is analyzed by the FEM. The effects of the thickness to radius ratio and type of mesh on the results are investigated in the simulation. The thickness to radius ratios selected are 0.002, 0.01, 0.1, and 0.2. In considering numerical accuracy as well as efficiency, numerical integration is carried out by using 2×2 Gauss points in the middle surface (an increased number of Gauss points, say, 3×3, may result in an overstiff system, which is called the shell locking phenomenon[13]). Table I summarizes the analytical solutions and the numerical results of the natural frequencies for the several lowest modes. It is evident that the error of the numerical results is reduced as the number of elements is increased. In addition, case 4 shows the natural frequencies of some torsional modes which can only be obtained by sufficiently fine meshes (i.e., meshes B and C).

TABLE I. Nondimensional natural frequencies $\Omega=\omega r_m/c_p$ of the thin spherical shell. ($E=1.9\times 10^{11}$ Pa, $\nu=0.3$, $\rho_s=7700$ kg/m^3; case 1: $h/r_m=0.002$; case 2: $h/r_m=0.01$; case 3: $h/r_m=0.1$; case 4: $h/r_m=0.2$.)

Case	Mode order n	Exact	Mesh A	Mesh B	Mesh C
1	1	0.0000	0.0000	0.0000	0.0000
1	2	0.7009	0.7103	0.7041	0.7026
1	3	0.8300	0.8904	0.8473	0.8395
2	1	0.0000	0.0000	0.0000	0.0000
2	2	0.7010	0.7104	0.7038	0.7028
2	3	0.8304	0.8912	0.8419	0.8403
2	4	0.8820	...	...	0.9145
3	1	0.0000	0.0000	0.0000	0.0000
3	2	0.7079	0.7190	0.7153	0.7101
3	3	0.8731	0.9460	0.9195	0.8855
3	4	1.0137	...	...	1.0592
4	1	0.0000	0.0000	0.0000	0.0000
4	2	0.7281	0.7393	0.7312	0.7292
4	3	0.9895	1.0526	0.9982	0.9846
4	2	1.1676	1.1930	1.1795	1.1766
4	4	1.3307	...	1.3585	1.3089

The mode shapes of the first natural mode (with multiplicity 5) of the spherical shell with the thickness to radius ratio 0.01 calculated by using SVD (based on the mesh type A) are shown in Fig. 5. It is observed from these figures that the spherical shell is deformed into a spheroidal shell. These calculated mode shapes will be compared with those of the containing thin spherical shell in the discussion of the coupled sound–structure system.

B. The spherical shell filled with a compressible fluid

In this section, a free vibration analysis is presented to explore the contributing factors that affect the interactions between the structure and the fluid.

First, the effect of thickness to radius ratio is investigated. Consider a spherical shell made of steel and filled with water. The material properties and physical dimensions are $r_m=1.0$ m, $E=1.9\times 10^{11}$ Pa, $\nu=0.3$, $\rho_s=7700.0$ kg/m^3, $\rho_f=1000.0$ kg/m^3, and $c=1460.0$ m/s. Three kinds of thickness to radius ratios, $h/r_m=0.002$, 0.01, and 0.2, are chosen for the numerical simulation. The results of the minimum singular values are plotted against the nondimensional natural frequency $\Omega=\omega r_m/c_p$ in Fig. 6 for the case of thickness to radius ratio 0.01. The natural frequencies of the first two natural modes of the shell, with and without the fluid loading, obtained independently from the

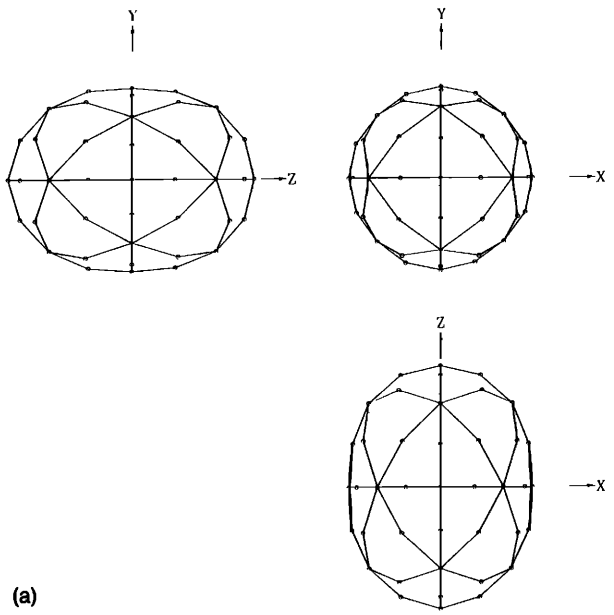

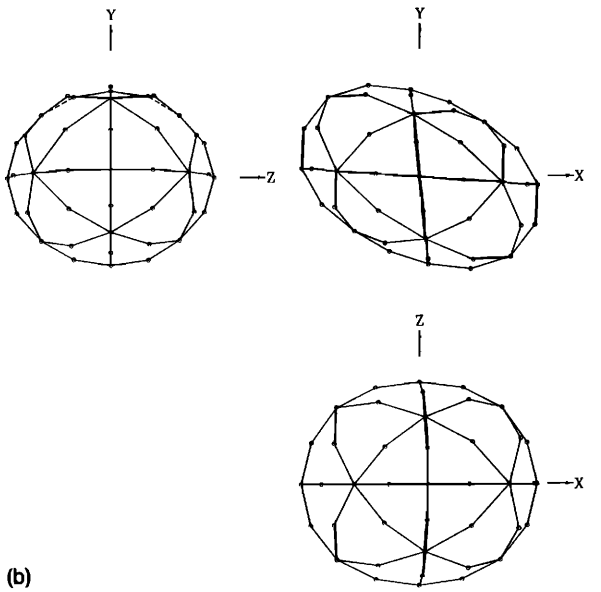

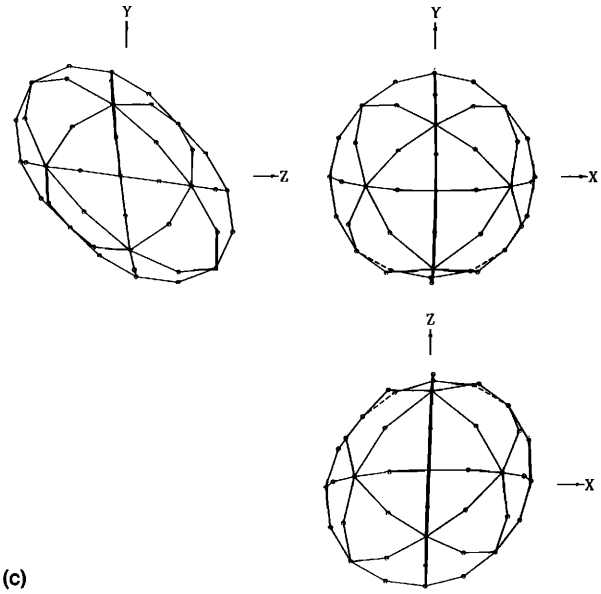

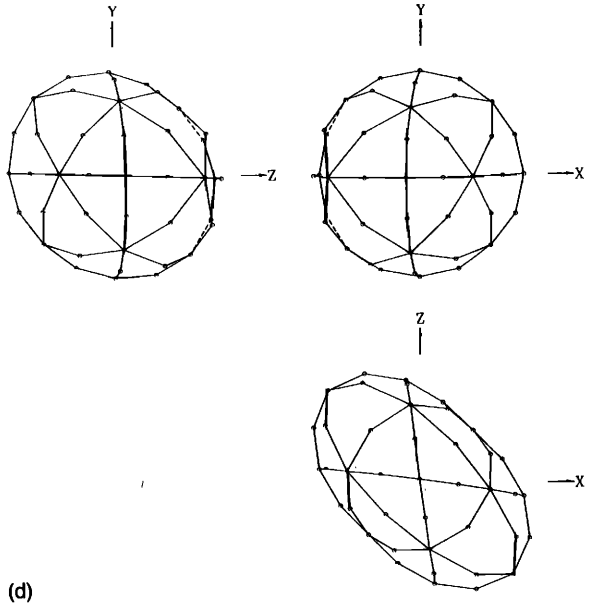

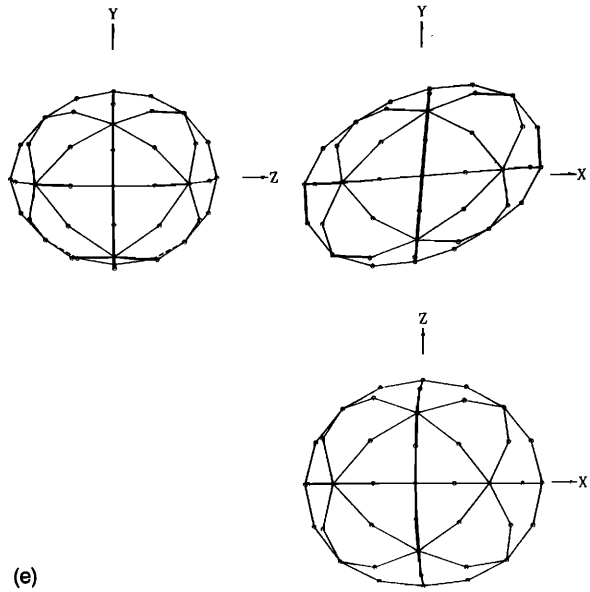

FIG. 5. The three-view diagrams of the normalized mode shapes corresponding to the first natural frequency of the spherical thin shell *in vacuo* ($h/r_m=0.01$, $E=1.9\times10^{11}$ Pa, $\nu=0.3$, $\rho_s=7700$ kg/m^3). (a) $\Omega=0.7072$; (b) $\Omega=0.7105$; (c) $\Omega=0.7111$; (d) $\Omega=0.7111$; (e) $\Omega=0.7121$.

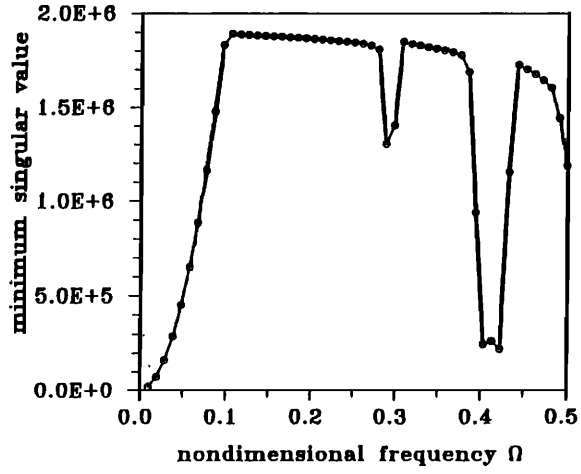

(a)

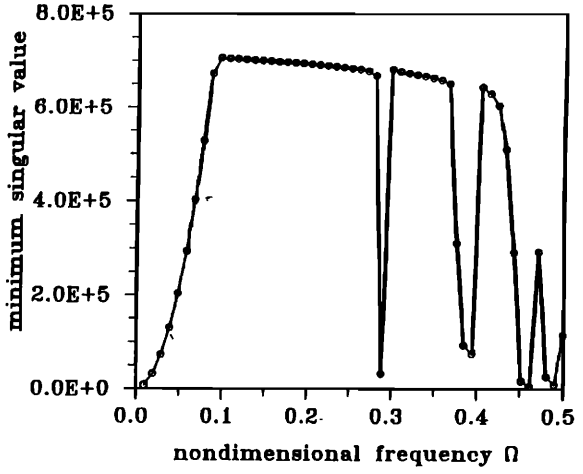

(b)

FIG. 6. Minimum singular values plotted against the nondimensional frequency Ω of the containing spherical thin shell ($h/r_m=0.01$, $E=1.9\times10^{11}$ Pa, $\nu=0.3$, $\rho_s=7700$ kg/m^3, $\rho_f=1000$ kg/m^3, $c=1460$ m/s). (a) Mesh type A; (b) mesh type B.

analytical and numerical methods are compared in Table II. From the results, it is observed that the natural frequencies of the coupled system are lower than those of the structure *in vacuo*. Significant decrease of natural frequencies occurs for very thin shell structures that interact strongly with the contained fluids. This can be attributed to the added mass effect resulting from the radiation reactance of the interior acoustic field.

The multiplicity of an eigenvalue of the coupled system can be determined by the number of singular values which are closer to zero in comparison with the others. In some cases, repeated eigenvalues spill over within a small interval of wave numbers. Great care has to be taken in determining the multiplicity of eigenvalues which may be the sum of the multiplicities of several proximate local minima within a small interval located by SVD. Sufficiently small step size of wave number is generally required for finding a complete set of multiple eigenvalues. For example, the singular values in the neighborhood of the first natural frequency (approximately 0.29) of the containing shell with the thickness to radius ratio 0.01, calculated by using the mesh type A, are shown in Fig. 7. It can be seen from the number of singular value dips, the multiplicity of this natural frequency is $1+1+2+1=5$. The mode shapes of the same case are shown in Fig. 8. Comparison of the mode shapes in Fig. 5 with those in Fig. 8 shows great resemblance of the shell responses, with and without the fluid loading.

TABLE II. Nondimensional natural frequencies $\Omega=\omega r_m/c_p$ of the thin containing spherical shell filled with water. ($E=1.9\times10^{11}$ Pa, $\nu=0.3$, $\rho_s=7700$ kg/m^3, $\rho_f=1000$ kg/m^3, $c=1460$ m/s; case 1: $h/r_m=0.002$; case 2: $h/r_m=0.01$; case 3: $h/r_m=0.2$.)

Case	Mesh type	Mode order n	Spherical shell		Coupled system	
			exact	numerical	exact	numerical
1	A	2	0.701	0.710	0.141	0.146
1	A	3	0.830	0.890	0.186	0.204
1	B	2	0.701	0.704	0.141	0.142
1	B	3	0.830	0.848	0.186	0.192
2	A	2	0.701	0.710	0.286	0.293
2	A	3	0.830	0.891	0.373	0.419
2	B	2	0.701	0.704	0.286	0.288
2	B	3	0.830	0.847	0.373	0.389
3	A	2	0.728	0.739	0.623	0.635
3	A	3	0.990	1.053	0.868	0.916
3	B	2	0.728	0.731	0.623	0.628
3	B	3	0.990	0.998	0.868	0.883

In addition to thickness to radius ratio, the effect of the material properties also plays an important role in the sound–structure interaction problems. In the following simulation cases, the thickness to radius ratio is maintained constant for comparing the interaction effects due to different kinds of fluids. Consider a containing spherical shell having the following material properties: $r_m=1.0$ m, $h/r_m=0.01$, $E=7.0\times10^{10}$ Pa, $\nu=0.33$, $\rho_s=2710.0$ kg/m^3. In order to evaluate interactions in a more quantitative manner, a coupling index[20] G ($=\rho_f c^2 S/\langle m\rangle V$, where $\langle m\rangle$ is the average structural mass per unit area, S is the surface area, and V is the volume) is calculated for each case. Five kinds of fluids corresponding to five different orders of coupling (see Table III) are chosen for the simulation. Among these five cases, the first three cases are for air of low temperature and low pressure, high temperature and low pressure, and high temperature and high pressure situations, respectively. The fluids of the last two cases are for pure water and mercury. The first two natural modes of the coupled systems are calculated for each case, by using the BEM–FEM algorithm. The analytical and numerical solutions of the natural frequencies of the shells with and without the fluid loading are compared in Table IV. As reflected by the coupling index, it is found that the interaction between the shell and the fluid of very low density and sound speed is almost negligible. On the other hand, for air of high temperature and high pressure in case 3, significant changes of natural frequencies occur. This suggests that preventive measures must be taken against the damages caused by strong sound–structure interactions

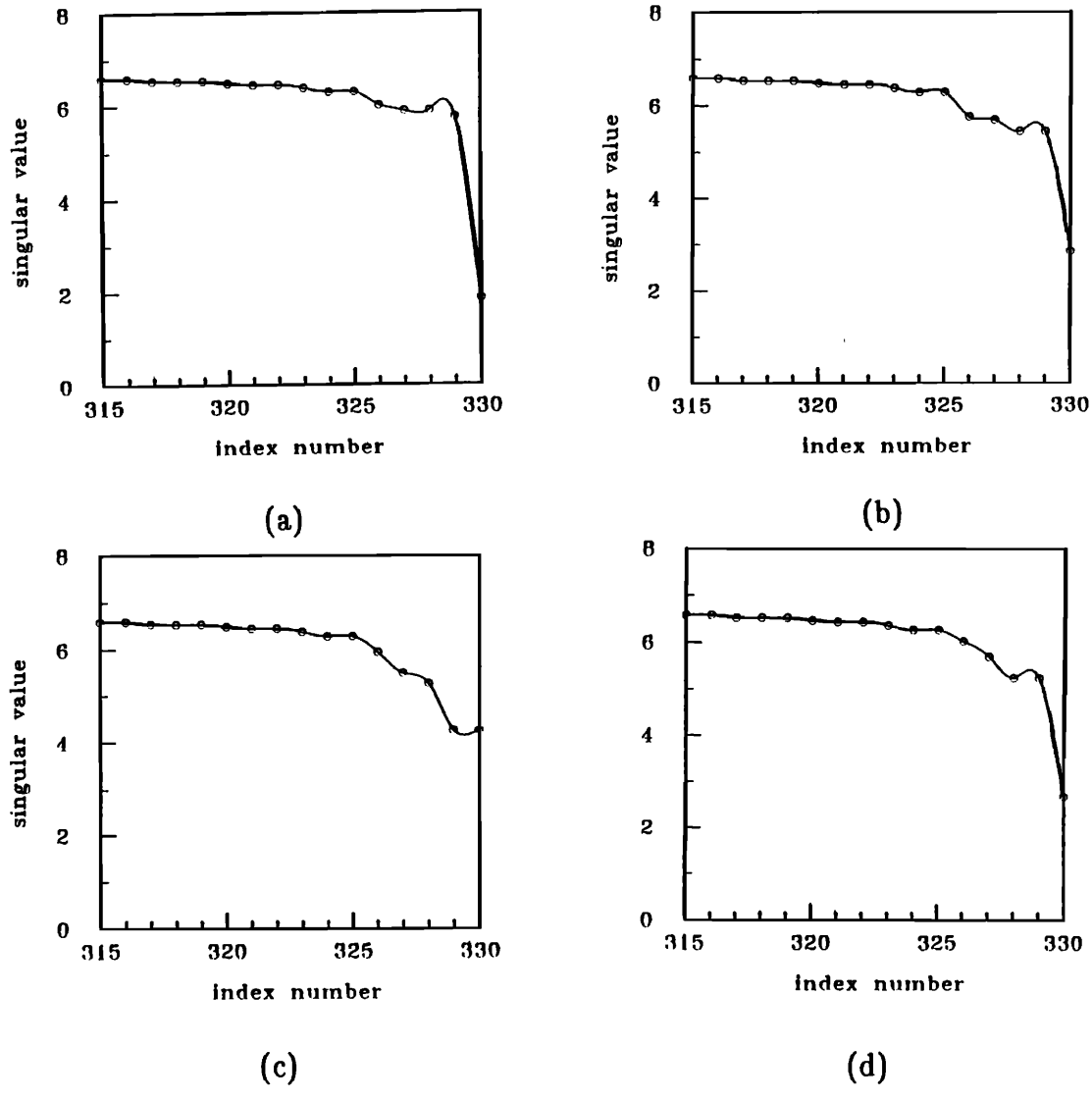

FIG. 7. Singular values of the containing thin spherical shell, corresponding to the first natural frequency. The y coordinate is plotted in the log scale. (a) $\Omega=0.2916$; (b) $\Omega=0.2930$; (c) $\Omega=0.2938$; (d) $\Omega=0.2941$. ($h/r_m=0.01$, $E=1.9\times10^{11}$ Pa, $\nu=0.3$, $\rho_s=7700$ kg/m^3, $\rho_f=1000$ kg/m^3, $c=1460$ m/s.)

for thin-walled structures containing high temperature and high pressure gases, such as ramjet engines, pressure vessels, and nuclear reactors.

In summary, the structure and fluid can be approximately treated as uncoupled systems for the situations of weak interactions. The natural frequencies of the fluid-loaded structure resemble the original structure *in vacuo*. On the other hand, the natural frequencies of the fluid-loaded structure are generally different from those of the original structure *in vacuo* for the situations of strong interactions. The shift of natural frequencies depends entirely on the degree of interactions, as reflected by the coupling index.

V. CONCLUSIONS

A hybrid numerical technique based on BEM and FEM has been developed to extract the natural frequencies and mode shapes of coupled fluid–structure systems. While use of this technique is not limited to simple geometries, the free vibrations of elastic thin spherical shells containing compressible fluids are investigated in a simulation because of the availability of analytical solutions. The physical insights derived from the simulation results can be summarized as follows.

For situations of strong interactions (e.g., a thin spherical shell containing a liquid or a gas of high temperature and high pressure), the dynamic characteristics of the coupled fluid–structure system can be significantly different from the original subsystems because of the fluid loading, while for situations of weak interactions, the coupled system can approximately be regarded as uncoupled systems. From the comparison of the natural frequencies of the shell with and without the fluid loading, it can be observed that the more strongly the structure interacts with the fluid, the larger the shifts of natural frequencies. For instance, the thickness to radius ratio is an important parameter in considering sound–structure interactions. Strong interactions may arise when a very thin shell is filled with a heavy fluid.

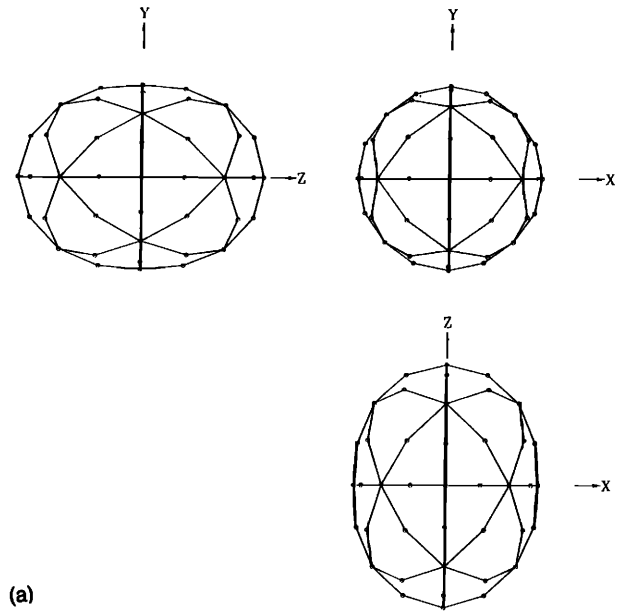

(a)

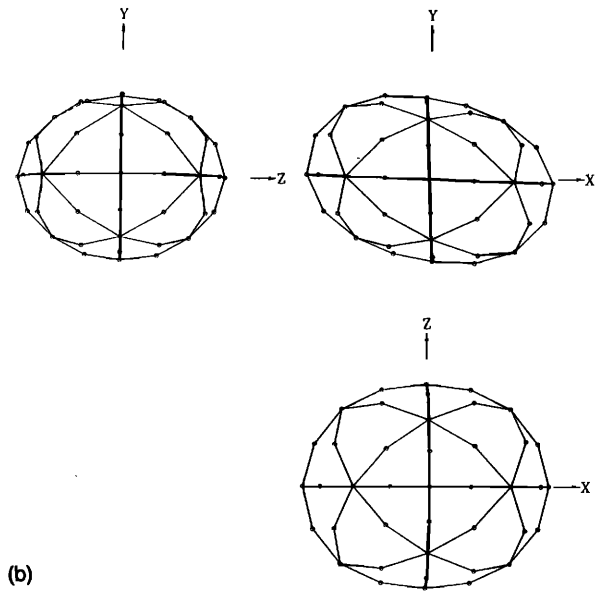

(b)

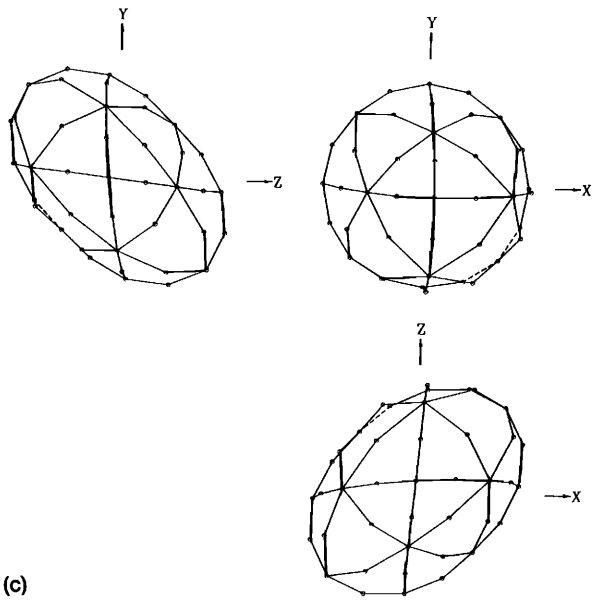

(c)

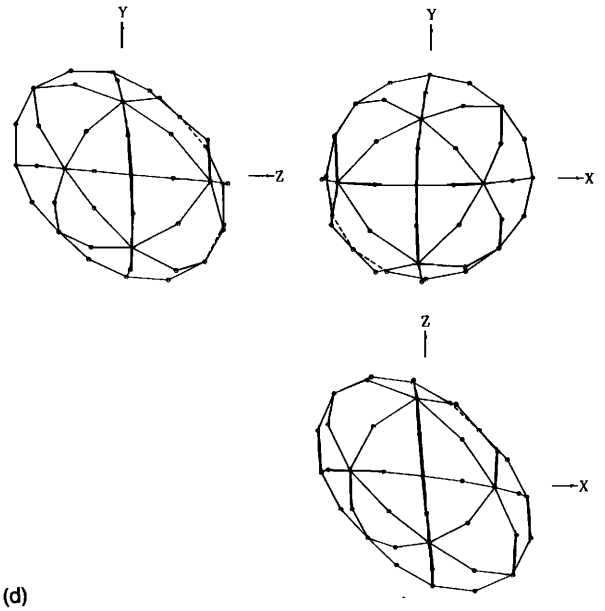

(d)

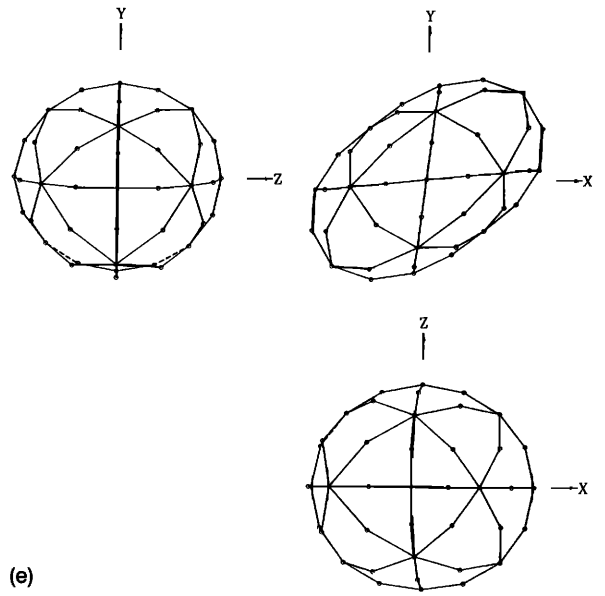

(e)

FIG. 8. The mode shapes of the first natural frequency of the containing thin spherical shell. (a) $\Omega=0.2916$; (b) $\Omega=0.2930$; (c) $\Omega=0.2938$; (d) $\Omega=0.2938$; (e) $\Omega=0.2941$. ($h/r_m=0.01$, $E=1.9\times10^{11}$ Pa, $\nu=0.3$, $\rho_s=7700$ kg/m^3, $\rho_f=1000$ kg/m^3, $c=1460$ m/s.)

TABLE III. Material properties and coupling indices $G=(\rho_f c^2/\langle m\rangle)S/V$ for cases 1–5. ($h/r_m=0.01$, $E=7.0\times10^{10}$ Pa, $\nu=0.33$, $\rho_s=2710$ kg/m^3.)

Case	ρ_f	c	G
1	1.21	346	5.4×10^3
2	1.21	520	1.2×10^4
3	32.31	520	3.2×10^5
4	998	1480	8.1×10^7
5	13 600	1450	1.1×10^9

Unlike the natural frequencies, the mode shapes of the structure do not seem to be markedly changed inasmuch as the sound–structure interaction is concerned. The mode shapes of the fluid-loaded structure remain rather similar to those of the structure *in vacuo* with only slight differences in the response amplitudes and torsional angles.

The method of SVD proves to be useful in searching for natural frequencies of the coupled system, although it appears somewhat computationally expensive. More efficient algorithms may be sought to deal with this nonstandard type of eigenvalue problems.

The numerical results illustrated in this paper are limited to only a few of the lower-order natural frequencies, not only because the computation requires enormous CPU time, which is beyond the computer resources available, but also because the FEM codes for the thin spherical shell developed in this study do not seem robust enough for extracting higher-order modes. In any event, one ought to recognize the fact that these types of numerical methods are suited for only low-frequency analyses because of the limitation of resolution, e.g., the discretization spacing should not be greater than one half of the wavelength, as a rule of thumb. If high-frequency applications are of interest, one should resort to alternative approaches, such as the statistical energy analysis (SEA).[21]

TABLE IV. Nondimensional natural frequencies $\Omega=\omega r_m/c_p$ of the thin containing spherical shell filled with different media. ($h/r_m=0.01$, $E=7.0\times10^{10}$ Pa, $\nu=0.33$, $\rho_s=2710.0$ kg/m^3; case 1: $\rho_f=1.21$ kg/m^3, $c=346$ m/s; case 2: $\rho_f=1.21$ kg/m^3, $c=520$ m/s; case 3: $\rho_f=32.31$ kg/m^3, $c=520$ m/s; case 4: $\rho_f=998$ kg/m^3, $c=1480$ m/s; case 5: $\rho_f=13\,600$ kg/m^3, $c=1450$ m/s.)

Case	Mode order n	Spherical shell		Coupled system	
		exact	numerical	exact	numerical
1	2	0.689	0.687	0.694	0.696
1	3	0.818	0.863	0.820	0.867
2	2	0.689	0.687	0.682	0.696
2	3	0.818	0.863	0.809	0.847
3	2	0.689	0.687	0.639	0.646
3	3	0.818	0.863	0.759	0.782
4	2	0.689	0.687	0.181	0.186
4	3	0.818	0.863	0.239	0.258
5	2	0.689	0.687	0.0514	0.0529
5	3	0.818	0.863	0.0683	0.0753

Quantitative approaches for interpreting resonance phenomena of coupled sound–structure systems with reference to the degree of interaction remain to be explored through numerical as well as experimental investigations in the future.

ACKNOWLEDGMENT

The work was supported by the National Science Council in Taiwan, Republic of China, under the project number NSC-80-0401-E009-13.

[1] J. J. Faran, "Sound scattering by solid cylinders and spheres," J. Acoust. Soc. Am. **23**, 405–418 (1951).
[2] M. C. Junger, "Sound scattering by thin elastic shells," J. Acoust. Soc. Am. **24**, 366–373 (1952).
[3] L. H. Chen and D. G. Schweikert, "Sound radiation from an arbitrary body," J. Acoust. Soc. Am. **35**, 1626–1633 (1963).
[4] O. C. Zienkiewicz, D. W. Kelly, and P. Bettess, "The coupling of the finite element method and boundary solution procedures," Int. J. Num. Eng. **11**, 355–375 (1977).
[5] D. T. Wilton, "Acoustic radiation and scattering from elastic structures," Int. J. Num. Meth. Eng. **13**, 123–138 (1978).
[6] S. W. Wu, "A fast, robust, and accurate procedure for radiation and scattering analyses of submerged elastic axisymmetric bodies," Ph.D. thesis, London University (1989).
[7] A. D. Pierce, *Acoustics* (McGraw-Hill, New York, 1981).
[8] G. F. Roach, *Green's Functions* (Cambridge UP, New York, 1982).
[9] P. K. Banerjee and R. Butterfield, *Boundary Element Methods in Engineering Science* (McGraw-Hill, New York, 1981).
[10] M. C. Junger and D. Feit, *Sound, Structures, and Their Interaction* (MIT, Cambridge, MA, 1972).
[11] H. Kraus, *Thin Elastic Shells* (Wiley, New York, 1967).
[12] A. H. Shah, C. V. Ramkrishnan, and S. K. Datta, "Three-dimensional and shell-theory analysis of elastic waves in a hollow sphere," J. Appl. Mech. **36**, 431–444 (1969).
[13] R. D. Cook, D. S. Malkus, and M. E. Plesha, *Concepts and Applications of Finite Element Analysis* (Wiley, New York, 1989).
[14] J. W. Bull, *Finite Element Applications to Thin-Walled Structures* (Elsevier Applied Science, New York, 1990).
[15] O. C. Zienkiewicz, R. I. Taylor, and J. M. Too, "Reduced integration technique in general analysis of plates and shells," Int. J. Num. Meth. Eng. **3**, 275–290 (1971).
[16] W. Weaver, Jr., and P. R. Johnston, *Finite Elements for Structural Analysis* (Prentice-Hall, Englewood Cliffs, NJ, 1984).
[17] I. C. Mathews, "Numerical techniques for three-dimensional steady-state fluid–structure interaction," J. Acoust. Soc. Am. **79**, 1317–1325 (1986).
[18] B. Noble and W. Daniel, *Applied Linear Algebra* (Prentice-Hall, Englewood Cliffs, NJ, 1988).
[19] J. S. Arora, *Introduction to Optimum Design* (McGraw-Hill, Singapore, 1989).
[20] F. Fahy, *Sound and Structural Vibration* (Academic, London, 1985).
[21] R. Lyon, *Statistical Energy Analysis of Dynamic Systems* (MIT, Cambridge, MA, 1975).